JATIS Journal of Astronomical Telescopes, Instruments, and Systems

RESEARCH PAPER

High-speed atomic oxygen irradiation of atomically thin graphene for astronomical applications

Kazuto Kashiwakura,[a] Ikuyuki Mitsuishi,[a,*] Midori Hirota,[a] Yoshimi Niwa,[a]
Yuzuru Tawara,[a] Ryo Kitaura,[a,b] Haruka Omachi,[c] Masahito Tagawa,[d]
Kentaro Nomoto,[e] Kazuyuki Tsuruoka,[e] Kenji Kawahara,[f] and Hiroki Ago[f]
[a]Nagoya University, Graduate School of Science, Nagoya, Japan
[b]National Institute for Materials Science, Research Center for Materials Nanoarchitectonics, Tsukuba, Japan
[c]Nagoya University, Integrated Research Consortium on Chemical Sciences, Nagoya, Japan
[d]Kobe University, Graduate School of Engineering, Kobe, Japan
[e]Research and Development Division, Ushio Inc., Yokohama, Japan
[f]Kyushu University, Global Innovation Center, Kasuga, Japan

ABSTRACT. The first results of high-speed atomic oxygen (AO) irradiation tests for atomically thin single-layer graphene sheets are presented as space environmental tolerance evaluation tests toward application in astronomy. The single-layer graphene sample was prepared without a metal coating, and high-speed AO irradiation tests were conducted with an averaged velocity of ~6 km/s using a laser-detonation AO beam source assuming a low Earth orbit (LEO) case. The Raman spectral features were examined before and after the tests with fluence values of 2×10^{15}, 2×10^{16}, 2×10^{17}, 2×10^{18}, and 2×10^{19} atoms/cm^2. It was found that there is no significant change in the observed D/G ratios for fluence up to 2×10^{17} atoms/cm^2. In contrast, the D/G ratios changed from 0.04 ± 0.03 to 0.8 ± 0.4 for 2×10^{18} atoms/cm^2 drastically in both the averaged value and 1-sigma range. Furthermore, the D/G ratio could not be measured beyond 2×10^{19}atoms/cm^2 because no peaks were observed in both the G and D bands, which suggests that the degradation occurs between 2×10^{17} and 2×10^{18} atoms/cm^2 and no graphene sheets exist after the 2×10^{19} atoms/cm^2 irradiation. Scanning electron microscopy images also support this conclusion in terms of the observed image contrast. Consequently, to protect the single-layer graphene sheets from erosion, a special treatment such as coating is needed to survive in an LEO for $\gtrsim$ a day.

© The Authors. Published by SPIE under a Creative Commons Attribution 4.0 International License. Distribution or reproduction of this work in whole or in part requires full attribution of the original publication, including its DOI. [DOI: 10.1117/1.JATIS.10.2.026006]

Keywords: graphene; X-ray astronomy; high-speed atomic oxygen; thin-film devices

Paper 23103G received Aug. 29, 2023; revised Feb. 28, 2024; accepted Apr. 5, 2024; published May 22, 2024.

1 Introduction

Thin-film devices have been used in a wide variety of ways not only as filters and sample support grids used in X-ray synchrotron radiation facilities and electron microscopes as ground-based applications but also as passive temperature-control devices and optical blocking filters on board mission payload systems as space-based applications.[1–3] For example, in the case of X-ray astronomy, instrumental sensitivity for detector and telescope systems is sometimes limited by filter transmission, particularly in the soft energy band below 1 keV. X-rays from astronomical objects, such as black holes, stars, galaxies, and clusters of galaxies, cannot be observed directly from the ground because they are absorbed by the atmosphere of the Earth. For this reason, the observation instruments are mounted on, for example, balloons, rockets, and satellites, to perform observations at altitudes unaffected by the atmospheric absorption. Thus, improvements in the instrumental sensitivity are crucial considering the lifetime of space missions, because soft X-ray observations ($\lesssim 1$ keV) are essential for understanding the mysteries of the Universe in a multi-scale structure from stellar systems to galaxies, clusters of galaxies and the large-scale structure of the Universe.[4–6]

---

*Address all correspondence to Ikuyuki Mitsuishi, mitsuisi@u.phys.nagoya-u.ac.jp

In X-ray astronomy, thin-film devices consist of, for example, a combination of a light metal and polymeric films such as aluminum and polyimide and their supporters to hold the free-standing filter structure.[1–3,7,8] The sensitivity of the filter depends on the thickness of the coating material and polymeric films and an open-area ratio basically limited by their physical properties, such as mechanical strength and processing techniques. As for the thickness of the plastic films, it varies from few tens to hundreds of nanometers. Thus, large-area thin filters with higher mechanical strength make it possible to realize high-sensitivity thin-film devices for future astronomical missions. Recently, carbon nanotube (CNT) thin filters with low-energy X-ray transparency, higher mechanical strength, and superior thermal conductance have been proposed for X-ray detectors in space.[9] The concept is to utilize superior optical and mechanical properties of CNTs and apply the CNT thin filters in large-area optical blocking filters to protect soft X-ray detectors from the intense optical light of the Sun in astronomical space missions. Bare and aluminum-coated small self-standing pellicles were fabricated successfully, and they exhibited their effectiveness in terms of X-ray transparency quantitatively as a potential innovative material.

In this study, as a new approach of replacing polymeric materials with a new material, we explored the possibility of atomically thin graphene to achieve ultimately high X-ray transparency for applications in astronomy. Graphene is also an allotrope of carbon composed of a monolayer of atoms arranged in a hexagonal lattice structure and known to possess outstanding physical properties, such as exceptionally high mechanical strength and electronic and thermal conductivity, which makes it an ideal material for filters. To verify whether graphene sheets can be applicable to thin filters in future space missions, we need to establish fabrication processes to realize possible large-area graphene-based filters that exhibit sufficient tolerance to survive severe space environments. As a first step of a space environmental tolerance evaluation test with applications in astronomy, we focused on tolerance against atomic oxygen (AO). AO is a major component of the atmosphere at altitudes of 200 to 500 km, and mission instruments on board rockets and satellites, particularly in a low Earth orbit (LEO), are sometimes supposed to be exposed to AO directly. In such a situation, AO is known to give rise to a variety of chemical and physical complex reactions with polymeric materials because the AO flow velocity is expected to be ~ 8 km/s corresponding to ~ 5 eV at an altitude of 500 km.[10] Thus, we evaluated the tolerance of uncoated bare graphene for high-speed AO for space applications.

In this paper, we report the irradiation test results for single-layer graphene films under high-speed AO irradiation simulating the space environment. Section 2 describes the graphene sample information and the details of the tests, Sec. 3 describes the evaluation method and results, and Sec. 4 summarizes the results.

2 Experimental Method

This section describes the preparation of the graphene samples and the experimental method employed in high-speed AO irradiation tests.

2.1 Sample

The details of the sample information used in this study are described in this section. We used single-layer graphene (8-mm square) transferred onto a SiO_2/Si substrate (15-mm square) with a

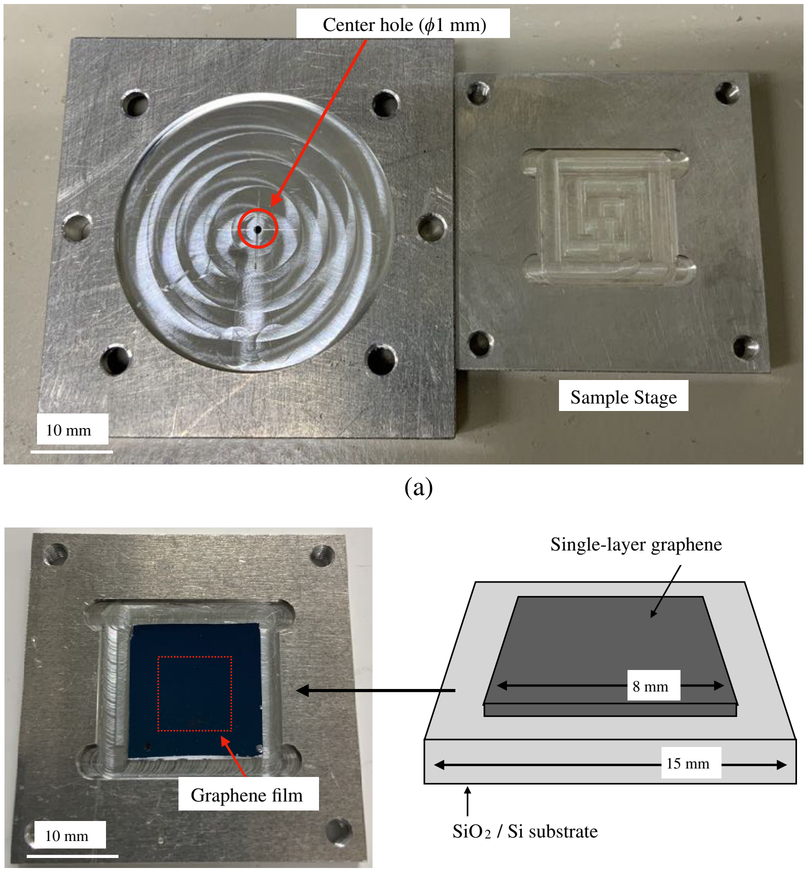

(a)

(b) (c)

Fig. 1 (a) Overview of the aluminum jigs. The top cover has a 1-mm diameter pinhole at the center to avoid the irradiation for edge parts of the graphene sheets and clarify the irradiation area. Graphene sample on (b) a $\mathrm{SiO_2/Si}$ substrate on the sample stage and (c) its schematic diagram.

thickness of 625 μm. The single-layer graphene was formed on a Cu/sapphire substrate through chemical vapor deposition,[11] followed by the coating and baking of a polymethyl methacrylate (PMMA) protective film at a temperature of 180°C for 1 min. Thereafter, the following processes were carried out: etching of the Cu/sapphire substrate using ammonium persulfate (0.1 M), pure water rinsing, transferring onto the $\mathrm{SiO_2/Si}$ substrate, and finally removing the PMMA film using acetone. To reduce the PMMA residue, the PMMA removal process was performed at a temperature of 60°C for 30 min. In addition, to prevent erosion from the edges of the graphene sheets and clarify the irradiation area, the sample was irradiated by high-speed AO on an aluminum jig (50 mm square, 6 mm thick) that had a 1-mm-diameter pinhole at the center, as shown in Fig. 1.

2.2 High-Speed AO Irradiation Tests

This section summarizes the experimental setup and conditions for high-speed AO irradiation tests.

In this study, we investigated tolerance for high-speed AO in a low-orbit case with an altitude of $\sim$500 km corresponding to a relative velocity of $\sim$8 km/s and a kinetic energy of $\sim$5 eV. To achieve our purposes, a laser-detonation AO beam source at Kobe University[12] was used for the high-speed AO irradiation simulations. The expected AO fluence depends strongly on a variety of factors of launch conditions and space environments, such as the location of instruments, the operational altitude of the spacecraft, and a solar activity. For example, in the case of a previous X-ray satellite, *Hitomi* (ASTRO-H), the required AO fluence for the thin-film devices consisting

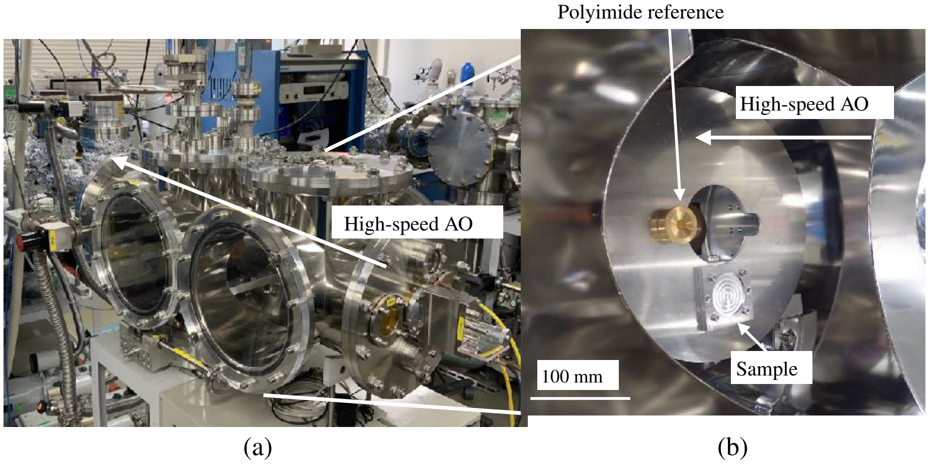

Fig. 2 (a) Overview of the high-speed AO irradiation test facility[12] and (b) the single-layer graphene sample and a polyimide reference in the sample chamber.

of polyimide films was $\sim 5 \times 10^{20}$ atoms/cm^2.[2] Therefore, an aluminum coating was applied on the polyimide films to impart high tolerance to them to withstand for such a high fluence, as serious damages to the polyimide film following high-speed AO irradiation were reported and expected.[13–15] Considering the fact that high-speed AO tolerance for single-layer graphene has not been investigated in detail even though AO adsorption is known to occur on graphene in not so high-speed AO environments,[16–18] in this study, we evaluated the behaviors of single-layer graphene by irradiating high-speed AO without a metal coating. Thus, high-speed AO was irradiated with fluence values of 2×10^{15}, 2×10^{16}, 2×10^{17}, 2×10^{18}, and 2×10^{19} atoms/cm^2. The fluence value of 2×10^{15} atoms/cm^2 corresponds to the minimum value in our experimental setup. The energy distribution during irradiation is estimated by measuring the time of flight (TOF) of ionized high-speed AO using a quadrupolar mass spectrometer located downstream of the high-speed AO beam line. The velocity was converted from the TOF and the averaged velocity was calculated to be ~ 6 km/s. The fluence was determined using the mass loss data of a reference polyimide sample, and the flux was 1.8×10^{15} atoms/cm^2/shot. These tests were conducted under a vacuum level of $\sim 10^{-6}$ Pa and almost vertical ($\sim 83^\circ$) AO impact was expected for all of the samples during the irradiation tests.[19] The beamline and inside of the sample chamber are shown in Fig. 2.

3 Analysis and Results

This section describes the evaluation method of the samples before and after the tests and presents the test results.

3.1 Analysis

To evaluate the status of single-layer graphene before and after high-speed AO irradiation, we used a Raman spectrometer that is usually employed to evaluate the molecular and crystal structures of carbon materials, such as graphite, CNT, and graphene and a scanning electron microscope (SEM) to observe the surface condition. The Raman spectroscopy measurements were performed using a Renishaw instrument with an exposure time of 3 s, laser power of 5%, and wavelength of 532 nm. Because the laser light is blocked near the edge of the jig aperture, the measurements were performed at the 1 mm center aperture, and their averaged value was adopted for certain points as the initial condition before the tests. Mapping measurements were also performed to estimate an averaged value and a (1-sigma) spatial variation before and after the tests under the identical conditions as described above in the central 200 μm $\times$ 200 μm with a pitch of 6 to 10 μm.

We extracted the G and D band intensities through a fitting procedure, individually assuming a single Gaussian function in each Raman spectrum, and finally focused on a D/G ratio, which is an indicator usually used to quantify the degree of disorderliness and structural defects present in carbon materials. The G band ($\sim$1580 cm^{-1}) is the primary mode in graphene caused by a planar molecular motion, whereas the D $\sim$1350 cm^{-1} band is activated by disorderliness and defects. Thus, the ratio increases with decreasing structural quality of the graphene sample. As supplementary data, the intensity of the 2D mode, which also results from the characteristic mode of graphene, was also obtained as in previous studies on carbon materials. The 2D band intensity is also expected to decrease in a decreasing graphene structure. The SEM observations were performed using a JEOL SEM system with a magnification of ×70 at 2.00 kV.

3.2 Results

Some of the typical observed Raman spectra for each high-speed AO irradiation fluence are presented shown in Fig. 3. The observed spectra with fluence values of 2×10^{15}, 2×10^{16}, and 2×10^{17} atoms/cm^2 are very similar to each other, whereas the behavior of the 2×10^{18} atoms/cm^2 case is found to be different from the others, and no line features are seen for the 2×10^{19} atoms/cm^2 case. As for the cases with fluence values of 2×10^{15}, 2×10^{16}, and 2×10^{17} atoms/cm^2, very weak D band intensity was detected, whereas relatively very strong G band intensity was confirmed. In the 2×10^{18} atoms/cm^2 case, the contrast between the D and G bands becomes much smaller, which suggests that a significant change in terms of the D/G ratio occurs in the fluence values from 2×10^{17} to 2×10^{18} atoms/cm^2. As for the 2D band, emissions were detected except for the 2×10^{19} atoms/cm^2 case, although the relative intensities of the D and G bands changed drastically. The observed Raman spectra with the best fit models are shown in Fig. 6 of Appendix.

Next, we extracted each intensity of each band in each Raman spectrum and found that the D/G ratios before and after the high-speed AO irradiation changed from 0.02 ± 0.01 to 0.02 ± 0.01, 0.03 ± 0.02 to 0.02 ± 0.01, and 0.04 ± 0.03 to 0.05 ± 0.03 for 2×10^{15}, 2×10^{16}, and 2×10^{17} atoms/cm^2, respectively. Thus, we conclude that there are no significant changes. In contrast, the D/G ratio before and after the high-speed AO irradiation changed from 0.04 ± 0.03 to 0.8 ± 0.4 for 2×10^{18} atoms/cm^2 drastically in both the averaged value and 1-sigma range. Furthermore, the D/G ratio could not be measured following the 2×10^{19} atoms/cm^2 high-speed AO irradiation because no peaks were observed in both the G and D bands, which suggests that very few graphene sheets exist following the 2×10^{19} atoms/cm^2 irradiation. We confirmed that the behavior of the 2D band is similar to that of the G band. The observed D/G ratios are depicted and summarized in Fig. 4 and Table 1, respectively. Consequently, to prevent the single-layer graphene sheets from erosion, a special treatment such as coating is needed to survive in the LEO for $\gtrsim$ a day.

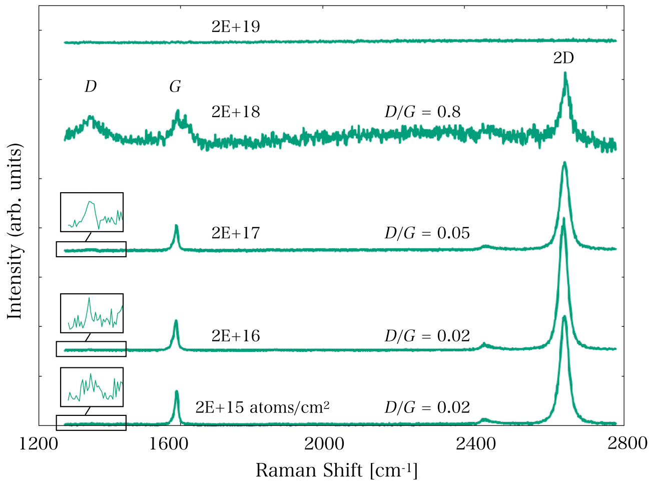

Fig. 3 Raman spectra of representative points for each fluence (2×10^{15} to 2×10^{19} atoms/cm^2). The spectral intensity has been corrected for clarity.

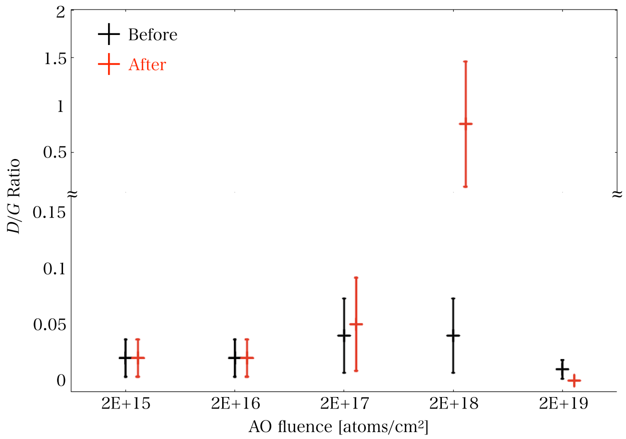

Fig. 4 *D*/*G* ratios before and after the high-speed AO irradiation tests as a function of the high-speed AO fluence. The ratio after the 2×10^{19} atoms/cm^2 irradiation was not plotted because the *G* and *D* bands were not observed.

Table 1 Summary of the *D*/*G* ratios for each fluence obtained by Raman spectroscopy before and after the high-speed AO irradiation tests. The ratio is not listed for that fluence because the *G* and *D* peaks were not observed after the 2×10^{19} atoms/cm^2 irradiation. The 1-sigma ranges were estimated based on Raman mapping measurements.

	D/*G* ratio	
AO fluence (atoms/cm^2)	Before	After
E+15	0.02 ± 0.02	0.02 ± 0.01
E+16	0.03 ± 0.02	0.02 ± 0.01
E+17	0.04 ± 0.03	0.05 ± 0.03
E+18	0.04 ± 0.03	0.8 ± 0.4
E+19	0.01 ± 0.01	—[a]

[a] No clear signal was seen.

Further, as in the case of the Raman spectroscopic results, there is a significant change in the contrast of the SEM images between the irradiated and unirradiated areas following the 2×10^{18} atoms/cm^2 irradiation. We could not see the difference in contrast up to the fluence value of 2×10^{17}atoms/cm^2; however, a clear contrast could be seen at larger fluence values of 2×10^{18} and 2×10^{19}atoms/cm^2. In particular, in the case of 2×10^{19} atoms/cm^2, the contrast of the irradiated area is consistent with that of the SiO_2/Si substrate area, suggesting that very few graphene sheets exist. The SEM images following the high-speed AO irradiation with fluence values of 2×10^{17}, 2×10^{18}, and 2×10^{19} atoms/cm^2 are presented in Fig. 5.

4 Summary

Thin-film devices play a key role in high-energy astrophysics, for example, X-ray astronomy, as passive temperature-control devices and optical blocking filters on board mission payload systems. Polymeric materials such as polyimide have been used, and sometimes thin-film devices limit sensitivity in terms of transmissivity, particularly at the soft X-ray energy range below 1 keV. Thus, we explored the possibility of replacing such polymeric materials with atomically thin graphene to achieve ultimately high X-ray transparency.

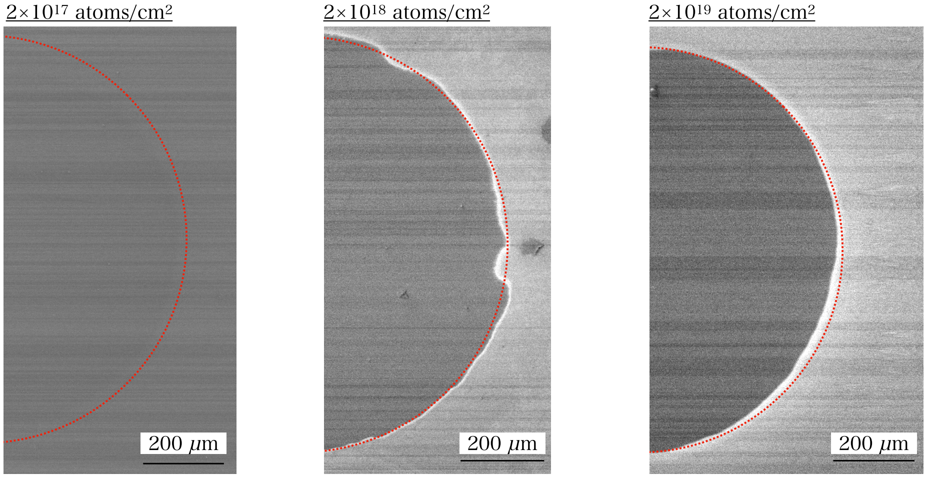

(a) (b) (c)

Fig. 5 SEM images after the high-speed AO irradiation with fluence of (a) 2×10^{17} (b) 2×10^{18}, and (c) 2×10^{19} atoms/cm^2. The red dotted line corresponds to the boundary between irradiated and unirradiated areas.

As a first step, we investigated the tolerance of single-layer uncoated graphene sheets for high-speed AO, expected to be exposed in the LEO. We prepared the single-layer graphene sample and conducted high-speed AO irradiation tests using the laser-detonation AO beam source. We examined the Raman spectral features before and after the tests with fluence values of 2×10^{15}, 2×10^{16}, 2×10^{17}, 2×10^{18}, and 2×10^{19} atoms/cm^2. It was found that the observed *D*/*G* ratios before and after the high-speed AO irradiation were from 0.02 ± 0.01 to 0.02 ± 0.01, 0.03 ± 0.02 to 0.02 ± 0.01, and 0.04 ± 0.03 to 0.05 ± 0.03 for 2×10^{15}, 2×10^{16}, and 2×10^{17}atoms/cm^2, respectively, and we conclude that there are no significant changes. However, the *D*/*G* ratios changed from 0.04 ± 0.03 to 0.8 ± 0.4 for 2×10^{18} atoms/cm^2 drastically in both the averaged value and 1-sigma range. Furthermore, the *D*/*G* ratio could not be measured following the 2×10^{19} atoms/cm^2 high-speed AO irradiation because no peaks were observed in both the *G* and *D* bands, which suggests that the degradation occurs between 2×10^{17} and 2×10^{18} atoms/cm^2 and very few graphene sheets exist following the 2×10^{19} atoms/cm^2 irradiation. The SEM images also support this conclusion because there is no significant difference in the image contrast between the irradiated and unirradiated areas up to the 2×10^{17} atoms/cm^2 case, and no evidence of the existence of the graphene sheets is seen in the 2×10^{19} atoms/cm^2 case. Consequently, to prevent the single-layer graphene sheets from erosion, a special treatment such as coating is needed to survive in the LEO for $\gtrsim$ a day. The details of the impact of erosion on specific functions such as mechanical strength will be examined in future studies.

5 Appendix: Raman Spectra

The observed Raman spectra with fluence values of 2×10^{15}, 2×10^{16}, 2×10^{17}, and 2×10^{18} atoms/cm^2 with the best fit models are shown in Fig. 6 of Appendix.

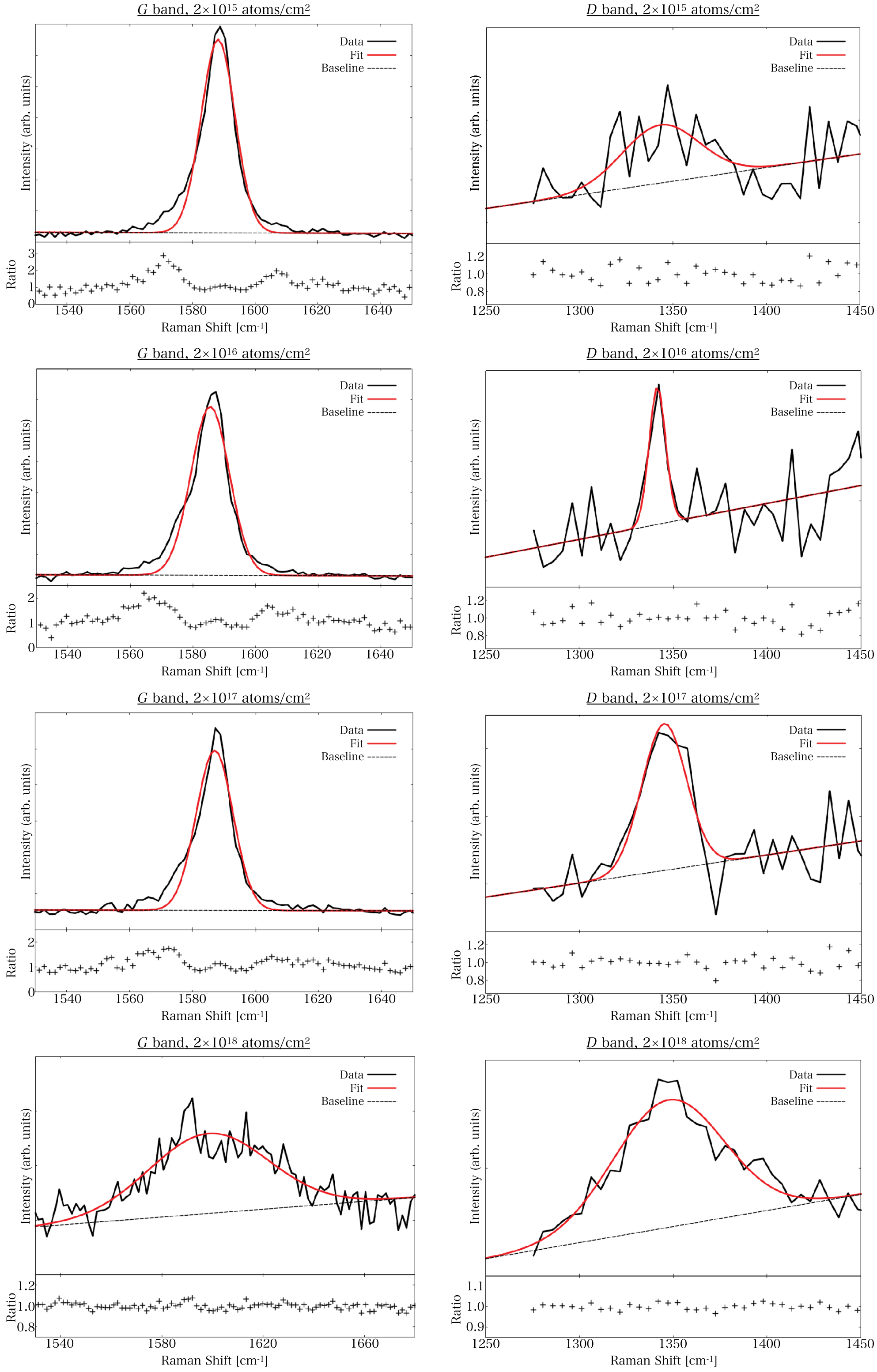

(a) (b)

Fig. 6 Observed Raman spectra for (a) *G* and (b) *D* band areas with fluence of 2×10^{15}, 2×10^{16}, 2×10^{17}, and 2×10^{18} atoms/cm^2 (from top to bottom).

Code and Data Availability

The datasets generated and/or analyzed during the current study are available from the corresponding author on reasonable request.

Acknowledgments

This study was financially supported by Grants-in-Aid for Scientific Research (KAKENHI) of the Japanese Society for the Promotion of Science (JSPS, Grant Nos. JP20K20920, JP22K18274: IM, JP23H05469: RK, JP21H05232, JP21H05233, JP23K17863: HA), Toshiaki Ogasawara Memorial Foundation (IM), Kondo Memorial Foundation (IM), Toyoaki Scholarship Foundation (IM), SCICORP (Grant No. JPMJSC2110: RK), and PRESTO (Grant No. JPMJPR20A2: RK).

References

1. P. J. Serlemitsos et al., "The X-ray telescope onboard Suzaku," *Publ. Astron. Soc. Jpn.* **59**, S9–S21 (2007).
2. Y. Tawara et al., "Development of ultra-thin thermal shield for ASTRO-H x-ray telescopes," *Proc. SPIE* **8147**, 814704 (2011).
3. M. Barbera, U. Lo Cicero, and L. Sciortino, "Filters for X-ray detectors on space missions," arXiv:2207.06781 (2022).
4. S. Takasao et al., "Investigation of coronal properties of X-ray bright G-dwarf stars based on the solar surface magnetic field-corona relationship," *Astrophys. J.* **901**, 70 (2020).
5. P. Kaaret et al., "A disk-dominated and clumpy circumgalactic medium of the Milky Way seen in X-ray emission," *Nat. Astron.* **4**, 1072–1077 (2020).
6. I. Mitsuishi et al., "Search for X-ray emission associated with the shapley supercluster with Suzaku," *PASJ* **64**, 18 (2012).
7. P. J. Serlemitsos et al., "The X-ray telescope on board ASCA," *Publ. Astron. Soc. Jpn.* **47**, 105–114 (1995).
8. B. D. Ramsey et al., "Optics for the imaging x-ray polarimetry explorer," *J. Astron. Telesc. Instrum. Syst.* **8**, 024003 (2022).
9. M. Barbera et al., "Carbon nanotubes thin filters for X-ray detectors in space," *Proc. SPIE* **12181**, 121814H (2022).
10. S. Packirisamy, D. Schwam, and M. H. Litt, "Atomic oxygen resistant coatings for low earth orbit space structures," *J. Mater. Sci.* **30**, 308–320 (1995).
11. H. Ago et al., "Epitaxial growth and electronic properties of large hexagonal graphene domains on Cu(111) thin film," *Appl. Phys. Express* **6**, 075101 (2013).
12. M. Tagawa et al., "Laser-detonation hyperthermal beam source applicable to VLEO environmental simulations," *CEAS Space J.* **14**, 757–765 (2022).
13. K. Yokota, M. Tagawa, and N. Ohmae, "Temperature dependence in erosion rates of polyimide under hyperthermal atomic oxygen exposures," *J. Spacecr. Rockets* **40**, 143–144 (2003).
14. B. A. Banks, K. K. de Groh, and S. K. Miller, "Low earth orbital atomic oxygen interactions with spacecraft materials (Invited Paper)," in *Materials for Space Applications*, M. Chipara et al., Eds., Vol. 851, p. 331, National Aeronautics and Space Administration (2005).
15. W. Zhao et al., "Erosion of a polyimide material exposed to simulated atomic oxygen environment," *Chin. J. Aeronaut.* **23**(2), 268–273 (2010).
16. N. A. Vinogradov et al., "Impact of atomic oxygen on the structure of graphene formed on Ir(111) and Pt(111)," *J. Phys. Chem. C* **115**(19), 9568–9577 (2011).
17. M. Z. Hossain et al., "Chemically homogeneous and thermally reversible oxidation of epitaxial graphene," *Nat. Chem.* **4**, 305–309 (2012).
18. Ž. Šljivančanin et al., "Binding of atomic oxygen on graphene from small epoxy clusters to a fully oxidized surface," *Carbon* **54**, 482–488 (2013).
19. H. Li et al., "Insights into impact interaction between graphene and high-speed atomic oxygen for aerospace protection application," *Appl. Surf. Sci.* **609**, 155274 (2023).

Ikuyuki Mitsuishi is a lecturer at Nagoya University, Japan. He received his MS degree in 2009 and his PhD in 2012 from the University of Tokyo in physics on the developments of space X-ray optics and studies of astronomical objects, such as stars, the Milky Way Galaxy, starburst galaxies, and galaxy clusters. His current research interests include high angular resolution X-ray optics and thin-film graphene devices, which are widely applied in both ground-based and space instruments and the studies of astronomical objects, such as the Sun, stars, the Milky Way Galaxy, and clusters of galaxies.

Biographies of the other authors are not available.